The application of wide angle screen propagator to 2D and 3D depth migrations

Xiao-Bi Xie, Institute of Tectonics, University of California, Santa Cruz*
Chuck C. Mosher, ARCO Exploration and Production Technology, Plano, Texas
Ru-Shan Wu, Institute of Tectonics, University of California, Santa Cruz

Summary

The wide-angle screen propagator for acoustic wave has been used for fast and accurate depth migration. Compared with the conventional phase screen method, the wide-angle version can give more accurate phase and amplitude for models with large velocity contrast and wide propagation angles. In this study, the wide angle propagator is applied to 2D and 3D common shot prestack depth migrations of the SEG/EAEG Salt Model. The model shows a number of challenging features to migration algorithms, e.g., strong velocity contrast and steep structures. Numerical results show that the new propagator gives significant improvements for imaging sub-salt structures.

Introduction

The phase screen method is based on the one way wave equation theory. It can be used as a high efficiency propagator for seismic migration (Stoffa *et al.*, 1990; Wu and Xie, 1994). The derivation of screen method usually requires that the velocity perturbation is small or the incident angle is small. However, real models used in imaging practices may contain very large velocity contrasts. Under these situations, the conventional phase screen method can give correct phase only within a small scattering angle, and can not generate satisfactory results. Several attempts have been made to improve the wide angle capability of the screen method. The PSPI method (Gazdag and Sguazzero, 1984) uses multi-reference velocities and then generate the solution using interpolations. The Fourier finite-diference method (Ristow and Ruhl, 1994), wide angle improvement method (Xie and Wu, 1998, 1999) and the modified pseudo screen method (Jin, Wu and Peng 1998) all use finite-difference method to improve the screen solution. Using the Harmilton path integrals, de Hoop *et al.* (1998) gave a general formulation for screen method. Based on their formulation, the accurate solution can be obtained by summing higher order terms of series. Huang *et al.* (1998) suggested an extended local Retyov method to improve the screen solution.

In this paper, we will briefly describe the equations of the wide angle screen propagator by Xie and Wu (1998, 1999). Then we will give 2D and 3D depth migration examples for synthetic data sets using the wide angle propagator algorithm.

Brief description of the method

The propagating wave field $p(\mathbf{x}_T, z)$ can be expressed as a superposition of plane waves

$$p(\mathbf{x}_T, z) = \int d\mathbf{k}_T \psi(z, \mathbf{k}_T) e^{i\mathbf{k}_T \cdot \mathbf{x}_T} \qquad (1)$$

where $\mathbf{x}_T = (x, y)$ and z are transverse and depth coordinates, $\psi(z, \mathbf{k}_T)e^{i\mathbf{k}_T \cdot \mathbf{x}_T}$ is a plane wave component, ψ is the amplitude and $\mathbf{k}_T$ is the transverse wavenumber. The propagator for plane wave amplitude can be obtained by solving the equation on ψ (Xie and Wu, 1998, 1999)

$$\frac{\partial \psi(z, \mathbf{k}_T)}{\partial z} = i \left[k_{0z} - k_0 (\frac{\delta c}{c} *) - k_0 \frac{a \left[(\frac{1}{n} *) - 1 \right] \frac{k_T^2}{k_0^2}}{1 - b \left[1 + (\frac{1}{n^2} *) \right] \frac{k_T^2}{k_0^2}} \right] \psi(z, \mathbf{k}_T) \qquad (2)$$

where $k_0 = \omega / c_0$ is the background wavenumber, k_{0z} is the vertical component of k_0, $a = 0.5$ and $b = 0.25$ are Padé expansion coefficients, n is Fourier transform of the refraction index c_0/c, $c = c(\mathbf{x}_T, z)$ is the velocity, c_0 is the background velocity, and "$*$" denotes the convolution in wavenumber domain.

On the right hand side of the equation, there are three terms. The first term gives the phase shift solution, first two terms combined give the conventional phase screen solution. The last term modifies the phase screen solution for wide angle incidence and large perturbations.

Figure 1 compared the dispersion curves of different approaches. Shown in this figure are vertical wavenumber k_z versus transverse wavenumber $\mathbf{k}_T$ for a plane wave penetrating a slab with constant velocity. To show the accuracy with large velocity perturbation, we chose reference velocity as half of the true velocity. The velocity contrast $c/c_0 = 2.0$ (i.e., 100% velocity perturbations). The inner circle is the accurate dispersion curve. The outer circle is the dispersion curve in the background velocity, i.e. the phase shift solution. The dispersion curve from the phase screen method

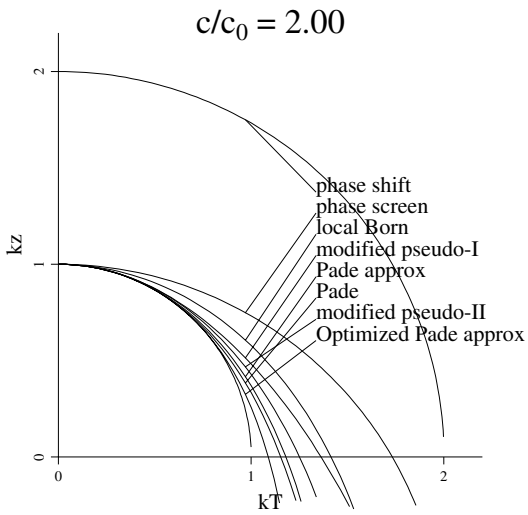

Figure 1: Comparison between dispersions from different propagators. The velocity $c = 2c_0$ (velocity perturbation is 100%). The vertical and horizontal coordinates are vertical and horizontal wavenumbers, Different curves indicate different approximations.

gives correct phase in the vertical direction but has large errors at wide angles. The wide angle version (marked with Padé approximation) using equation (2) gives much better results. As can be seen in the figure, if we optimize the parameters a and b, the result can be further improved.

Equation (2) can be solved using different approaches. A convolution in wavenumber domain can be replaced with a high efficiency multiplication in the space domain. A fast duel domain algorithm can be formed by calculating the first term in the wavenumber domain and the second and third terms in space domain (Xie and Wu, 1998). The process can be summarized into

$$p(\mathbf{x}_T, z_{i+1}) = P\{p(\mathbf{x}_T, z_i)\} \qquad (3)$$

With an iterative algorithm, the entirewave field in the $(\mathbf{x}_T, z)$ domain can be obtained. Both poststack and prestack migration involve back propagation of the received reflection seismograms downward. With time reverse, or equivalently, the conjugate of spectra of seismograms, the same forward propagator can be used to calculate back propagations. For common shot prestack migration, the imaging condition is

$$M_{shot}(\mathbf{x}_T, z) = \int p_s(\mathbf{x}_T, z, \omega) p_r^*(\mathbf{x}_T, z, \omega) d\omega \qquad (4)$$

$$M(\mathbf{x}_T, z) = \sum_{shots} M_{shot}(\mathbf{x}_T, z) \qquad (5)$$

where $p_s(\mathbf{x}_T, z, \omega)$ and $p_r^*(\mathbf{x}_T, z, \omega)$ are downward propagated wavefrom the source and downward propagated time reversed field from the receivers. $M_{shot}(\mathbf{x}_T, z)$ is the image from a singly shot, and $M(\mathbf{x}_T, z)$ is the stacked image from all shots.

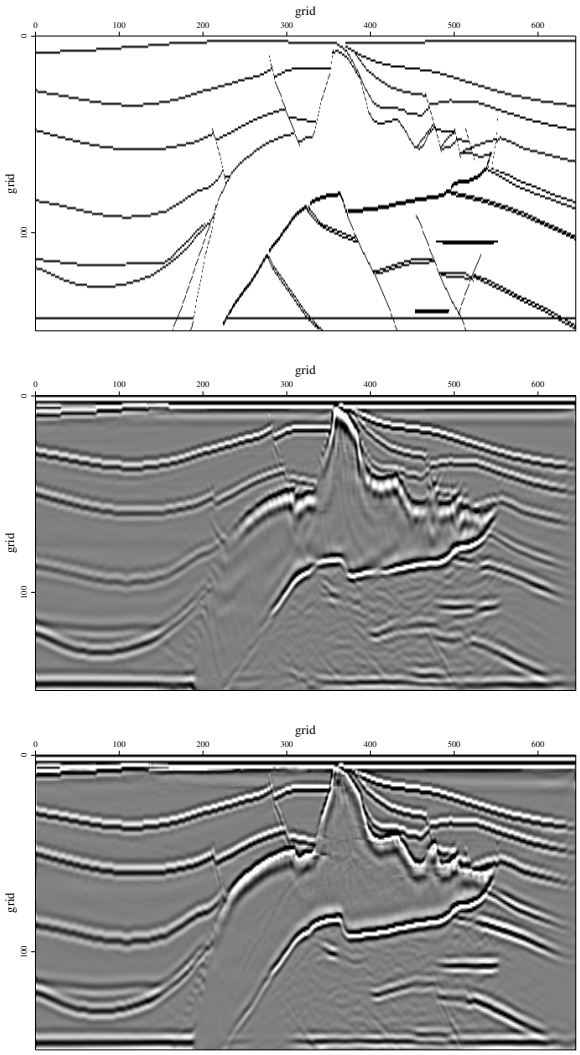

Figure 2: Comparison of 2D migration images using different methods. From top to bottom are reflection model, image using phase screen method, and image using wide angle screen method, respectively.

Test migration of 2D data set

Figure 2 shows the result of prestack depth migration of the 2D SEG/EAEG Salt Model. The synthetic data

set consists of 325 shots, and each shot has 176 traces. The trace length is 626 and the sampling rate is 8 ms. From the top to bottom are reflection model, image obtained using conventional phase screen method, and image using wide angle screen method. Compared with the phase screen result, the advantages of the wide angle method are apparent. It gives better image in several places, including a better bottom reflector, better images for steep structures above and below the salt body, more accurate upper and lower boundaries for the salt, etc.

Depth migration of 3D data set

Figure 3 shows the result of applying shot record migration with the wide angle screen correction for the 3D SEG/EAEG Salt Model. The data were generated by Sandia National Laboratory as part of the Advanced Computational Technology Initiative (Ober *et al.*, 1997). The dataset consists of a 5 x 9 shot array (45 shots) into a 201 x 201 receiver grid with 20m receiver spacing. Shots are spaced 1000 m in X and Y, and were selected to cover approximately the same region as the SEG/EAEG Salt Model C3 subset (Aminzadeh *et al.*, 1997). The input data are sampled at 8 ms with record length 4 sec, and usable frequency bandwidth in the range 1 to 30 Hz.

The top panel of Figure 2 shows In-Line 242 (X=4820m) from the full velocity model, with Y coordinate ranging from 0 to 13500m. The middle panel shows the result of migrating and stacking the first 9 shots from the Sandia subset using a phase screen propagator, also centered on In-Line 242. The Y coordinate ranges from 620 to 10620m. The bottom panel shows the same In-Line with the migration using wide angle propagator. Even with only nine shots, significant improvements in sub-salt structure can be seen compared to the first order phase screen. In particular, sediment reflectors that terminate under the salt can be identified. Subsalt imaging for this model continues to be a challenge, but we expect to make significant improvements as we fine-tune the numerical implementation of the wide angle screen propagators.

Conclusions

The preliminary results from 2D and 3D shot gather depth migrations using the wide angle version of the screen method show some encouraging features. The future work will be focused on reducing the noise level and improving the image of sub-salt structure.

Acknowledgements

The supports from the Basic Energy Science Branch of the Department of Energy and from the WTOPI Research Consortium at UCSC are acknowledged. The facility support from the W.M. Keck Foundation is also acknowledged.

References

Aminzadeh, F., Brac, J, and Kunz, T., 1997, 3-D Salt and Overthrust Models, SEG/EAGE 3-D Modeling Series, No. 1

de Hoop, M.V., R.S. Wu and J.L. Rousseau, 1998, General formulation of screen methods for the scattering of acoustic waves, submitted to the *Wave Motion*.

Gazdag, J., and P. Sguazzero, 1984, Migration of seismic data by phase shift plus interpolation: *Geophysics*, **49**, 124-131.

Huang, L.J., M.C. Fehler and C.C. Burch, 1998, A hybrid local Born/Rytov Fourier migration method, *Mathematical Methods in Geophysical Imaging V, SPIE,* **3453**, 14-25.

Jin, S., Wu, R.S. and Peng, C., 1998, Prestack depth migration using a hybrid pseudo-screen propagator, *Expanded abstracts, SEG 68th Annual Meeting*, 1819-1822.

Ober, C. C., Oldfield, R. A., Womble, D. E. and Mosher, C. C., 1997, Seismic imaging on massively parallel computers, *Expanded Abstracts, SEG 67th Annual Meeting*, 1418-1421.

Ristow, D. and T. Ruhl, 1994 Fourier finite-difference migration, *Geophysics*, **59**, 1882-1893.

Stoffa, P.L., Fokkema, J.T., de Luna Freire, R.M., and Kessinger, W.P., 1990, Split-step Fourier migration, *Geophysics*, **55**, 410-421.

Wu, R.S. and Xie, X.B., 1994, Multi-screen backpropagator for fast 3D elastic prestack migration, *Mathematical Methods in Geophysical Imaging II, SPIE, 2301*, 181-193.

Xie, X.B. and R.S. Wu, 1995, A complex-screen method for modeling elastic wavereflections: Expanded abstracts, *Expanded Abstracts, SEG 65th Annual Meeting* 1269-1272.

Xie, X.B. and R.S. Wu, 1996, 3D elastic wave modeling using the complex screen method, *Expanded Abstracts, SEG 66th Annual Meeting*, 1247-1250.

Xie, X.B. and R.S. Wu, 1998, Improve the wide angle accuracy of screen method under large contrast, *Expanded abstracts, SEG 68th Annual Meeting*, 1811-1814.

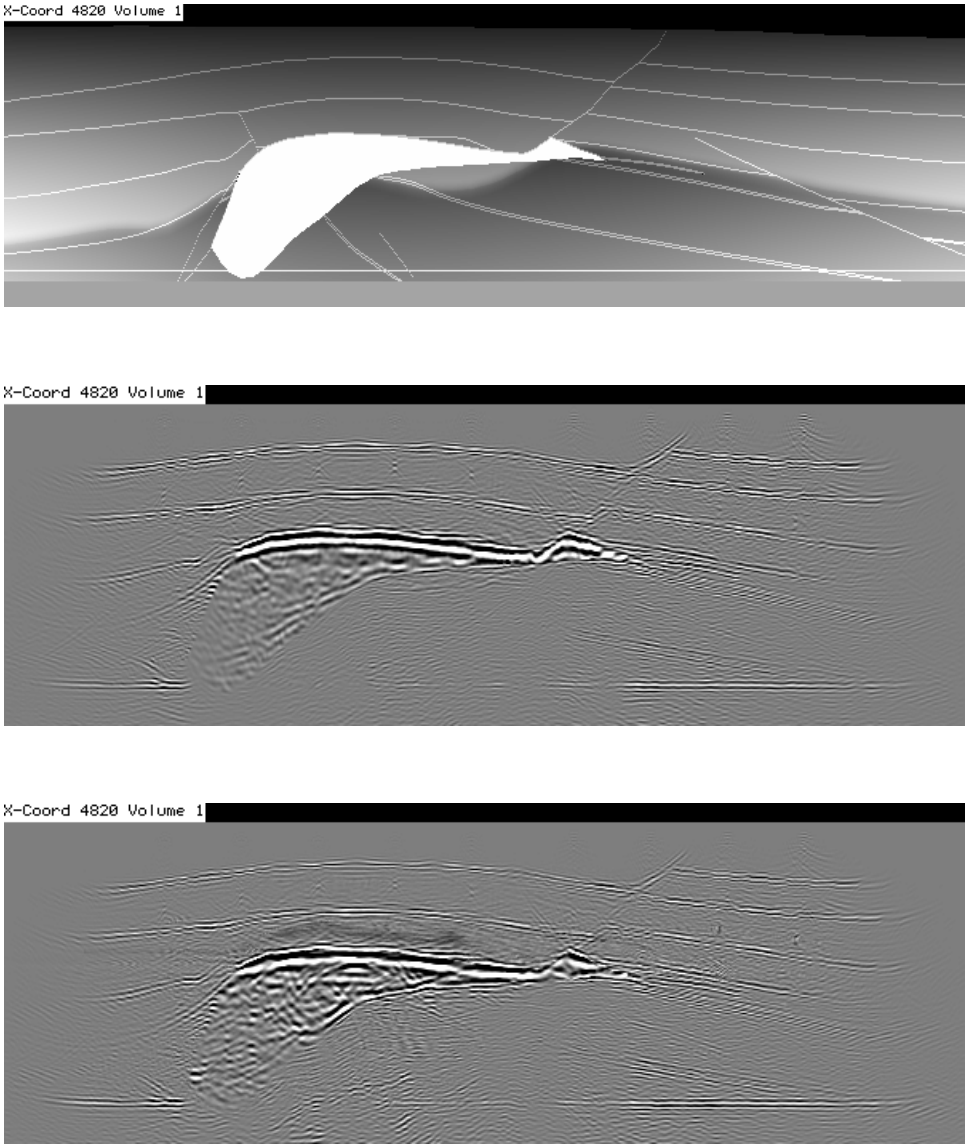

Figure 3: Comparison of 3D migration images using different methods. From top to bottom are velocity model, migration image using phase screen method, and image using wide angle screen method, respectively.